Vessel Recognition in Color Doppler Ultrasound Imaging

Ashraf A Saad

[1]Electrical Engineering Department, University of Washington

[2]Philips Healthcare, Ultrasound Division

Outline of the Work

1. Introduction
2. The Shape Decomposition Approach
3. Fringeline Tracking for Phase Unwrapping
4. Vessel Feature Generation and Selection
5. Vessel Classification

Introduction

- In the last few decades, ultrasound imaging systems have improved dramatically by offering high quality images.
- So far, ultrasound systems use very little knowledge of the content of images they acquire to optimize the acquisition and visualization processes of the images.
- The main consequence of this fact is that machine manipulation is still a tedious and time consuming task with too many controls to adjust.
- The goal of the work is to apply image analysis techniques to automate one aspect of the problem: segmenting blood vessels in ultrasound color Doppler images using high-level shape information.

Philips iU22 Ultrasound System

This system was used as a prototype platform for the research.

Screen Capture of an Ultrasound System

- The gray scale ultrasound image (top half) depicts the anatomy of body organs.
- The color Doppler image, overlaid on top of the grayscale image, depicts the blood flow velocity within blood vessels (the Carotid artery in this picture)
- The spectral Doppler scrolling image (bottom) depicts the variation of blood flow velocities with time (showing systole and diastole phases here)

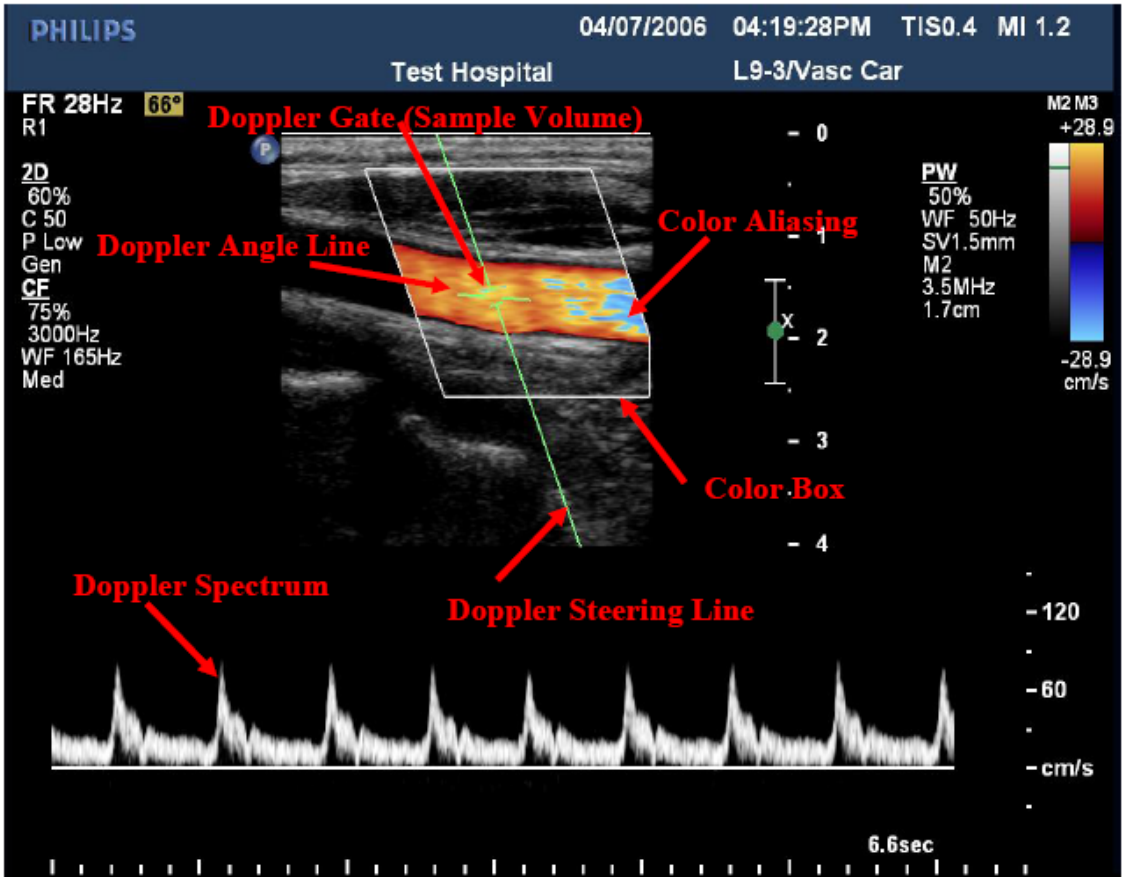

The user manipulates the graphical components to optimize the image.

Goal and Steps

Goal: Given a number of color Doppler ultrasound frames that contain one or more vessels, recognize all the specific vessels that exist in those images.

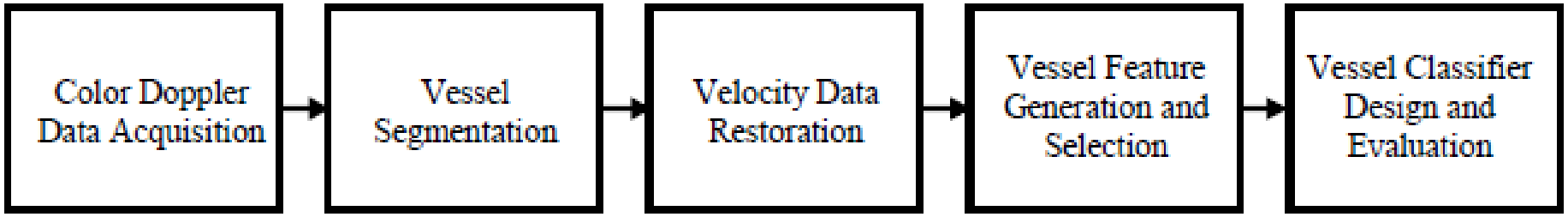

Shape Decomposition Approach

- Obtain a representation of the vessel that is suitable for extracting discriminative features
- Uses color Doppler ultrasound images that span one heart cycle
- The consecutive set of frames used is called a cineloop.
- The format of the color Doppler image is signed 8-bit pixels that form a color-coded representation of the directional mean velocity of each pixel.
- 30 frames per data set were captured.

Color Bleeding Artifact

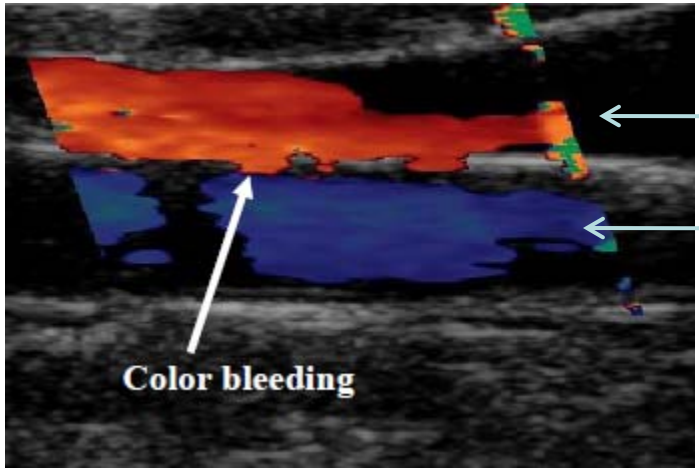

- Color bleeding artifact causes two or more distinct vessels to appear as if they are connected in certain points across their border.
- This is a primary source of difficulty in vessel segmentation.

Vessel Segmentation Approaches in the Literature

- Multi-Scale (multiple resolutions)
- Skeleton-Based
- Ridge-Based (treating grayscale images as elevation maps)
- Region-Growing
- Differential Geometry (models images as hyper surfaces and extracts features using curvature and crest lines)
- Matching Filters (convolves images with multiple filters)
- Mathematical Morphology
- Tracking
- AI and Model-Based

Multiple Resolutions: Image Pyramids

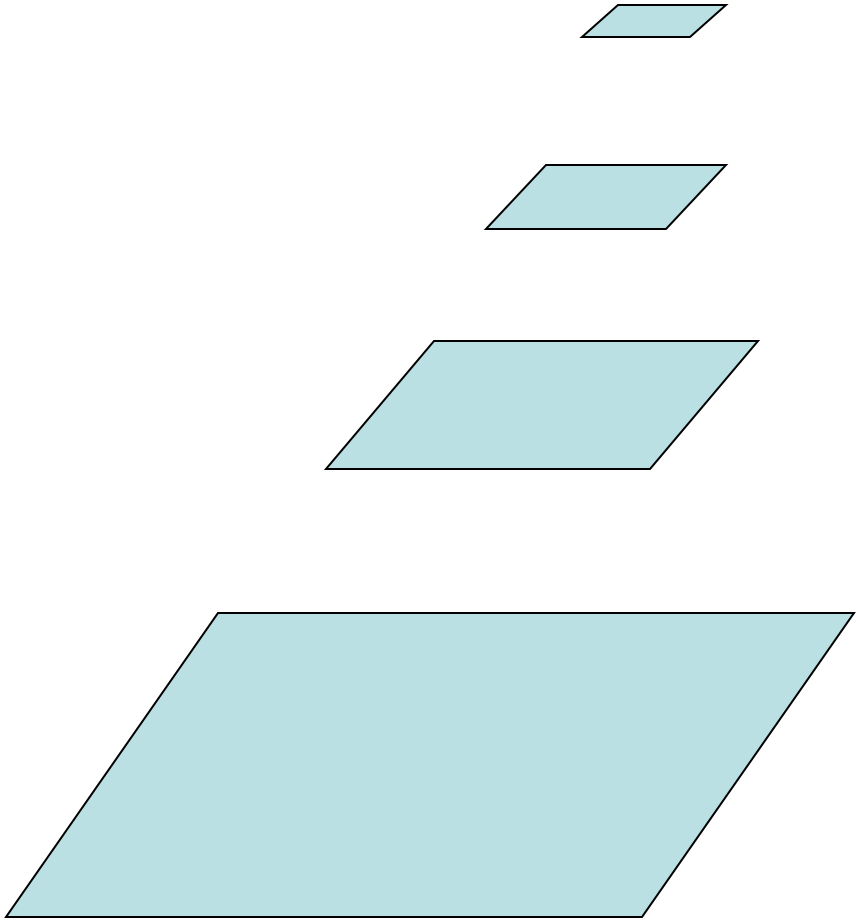

And so on.

3rd level is derived from the 2nd level according to the same funtion

2nd level is derived from the original image according to some function

Bottom level is the original image.

Example: Mean Pyramid

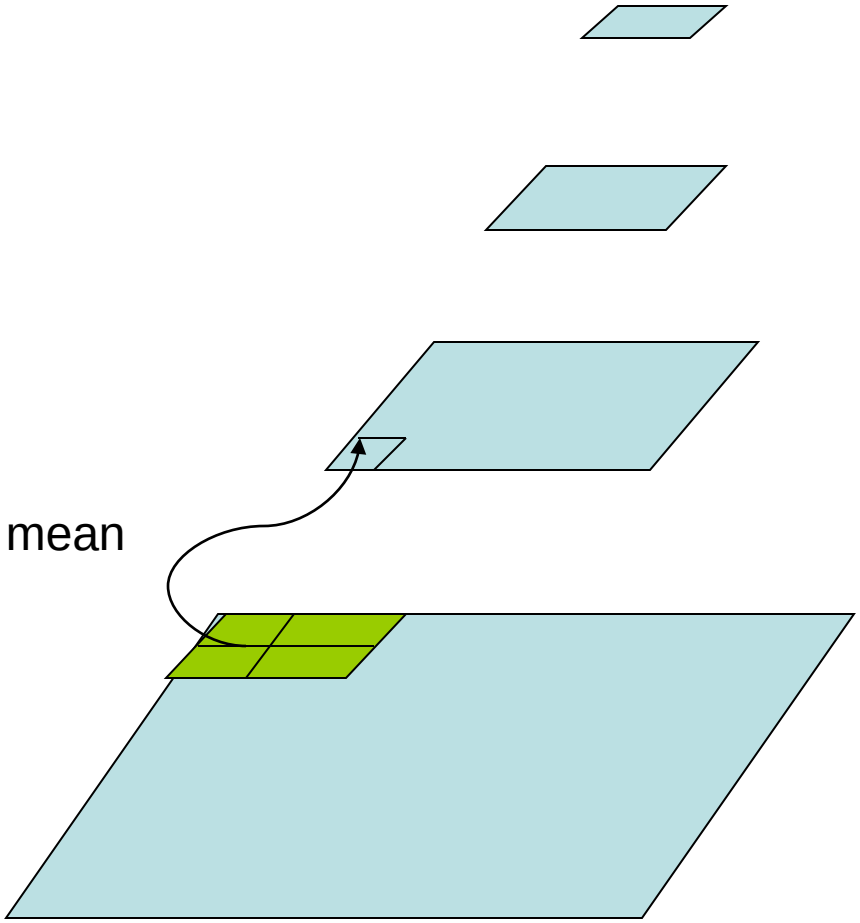

And so on.

At 3rd level, each pixel is the mean of 4 pixels in the 2nd level.

At 2nd level, each pixel is the mean of 4 pixels in the original image.

Bottom level is the original image.

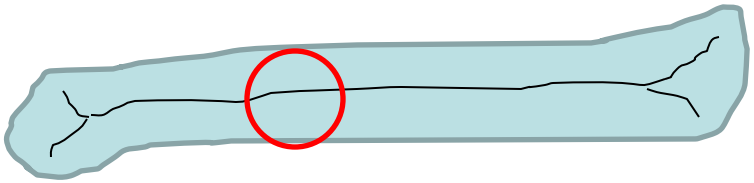

The skeleton or medial axis of a 2D shape is a set of points that are the centers of the set of maximal enclosed circles.

Vessels should have fairly long straight axes.

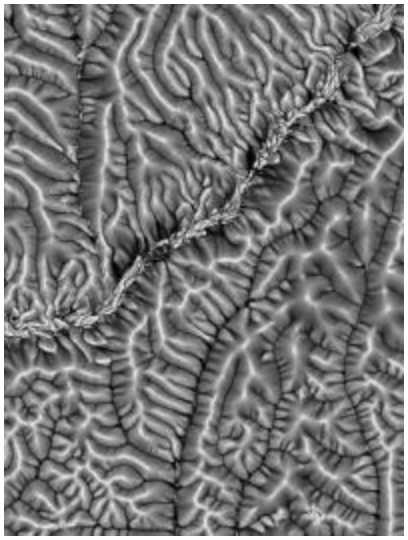

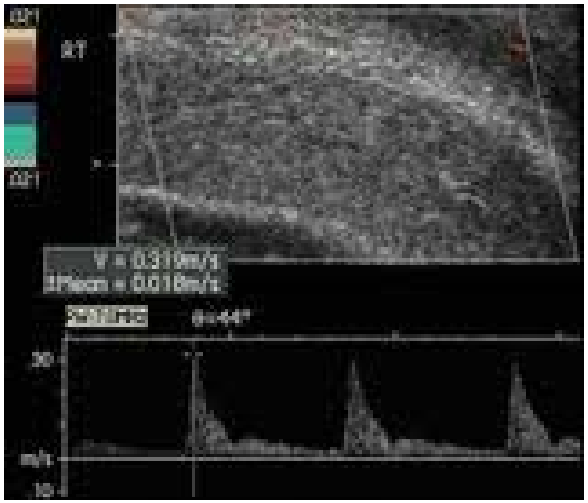

When a grayscale image is treated as an elevation map, the ridges are the lightest areas and the valleys the darkest areas.

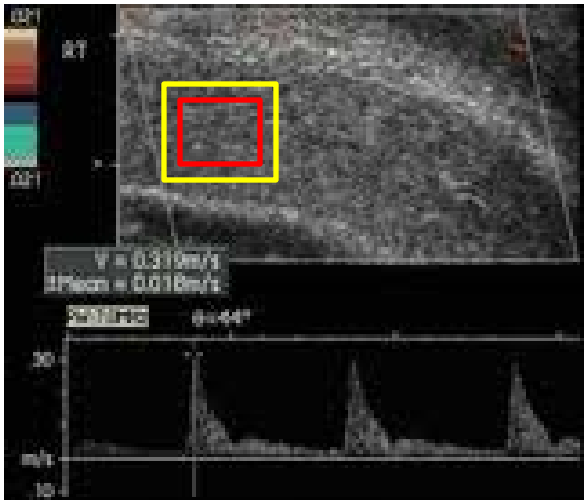

Region growing starts with a small region of an object to be detected, calculates its properties, and then performs statistical tests to decide whether or not to add adjacent pixels to “grow” the region.

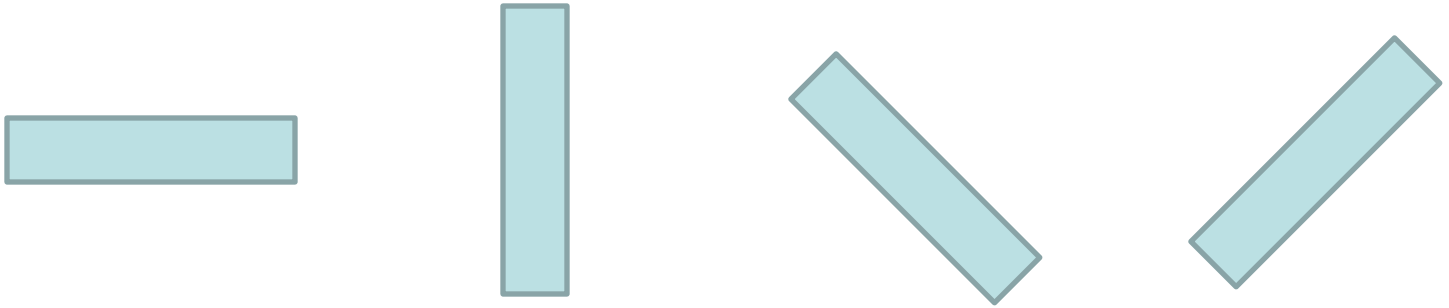

Mathematical morphology tries to fit structuring elements of different shapes and angles into the white areas of a binary thresholding of a graytone image.

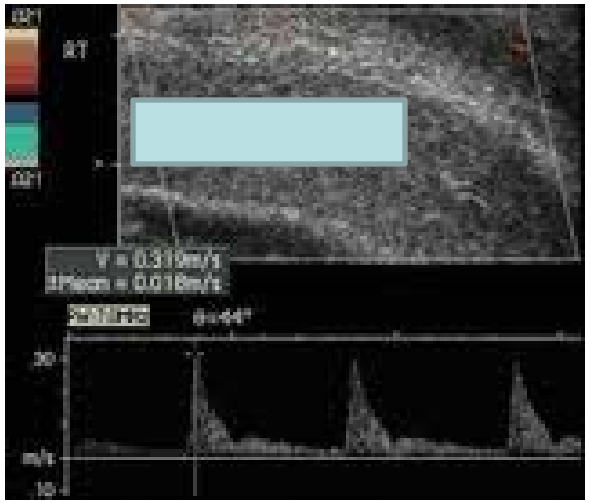

Shape Decomposition for Segmentation

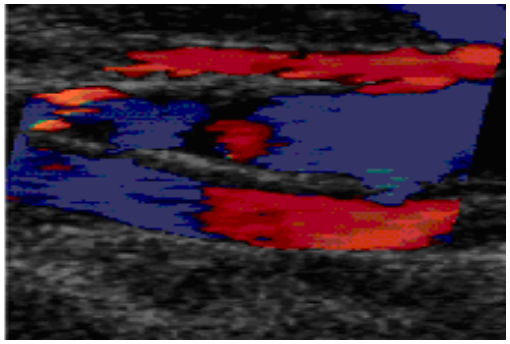

image representing a cineloop obtained as an average of all frames containing 4 vessels

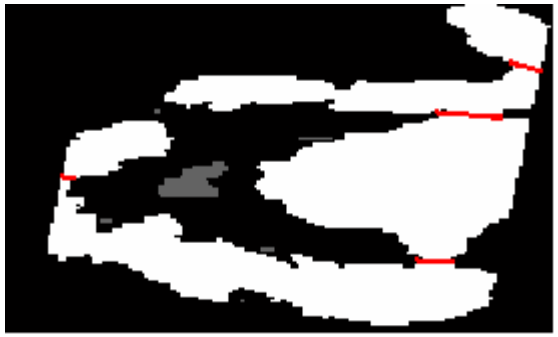

thresholded binary image with red lines representing the correct segmentation

Segmentation Algorithm Concepts

Def: A part-line is a line whose end points lie on the object boundary and is entirely embedded in the object as a separator of parts.

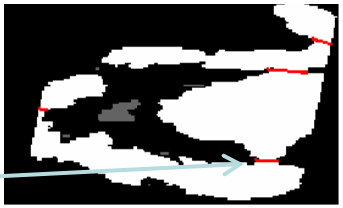

- Correct part-lines involve one (single-point part-line) or two (double-point part-line) negative curvature minima.
- Some negative curvature minima are due to noise
- Distinct vessel segments are mainly convex and elongated.
- When two adjacent parallel vessels are linked, the eccentricity of the resulting linked object will be less than that of at least one of the two original objects.

Shape Decomposition

```
1.  Shape Decomposition (object)
2.  {
3.      Detect concave points;
4.      Detect double-point part-lines;
5.      Filter double-point part-lines;
6.      Detect single-point part-lines;
7.      Filter single-point part-lines;
8.      Assign lists of concave points, double-point part-lines, and single-point part-lines
    to object
9.      Push object into stack;
```

```
10.   While (object stack is not empty)
11.   {
12.      Pop object and its lists from stack;
13.      if (double-point pat-line list is not empty)
14.      {
15.         Find best (maximum eccentricity) double-point part-line;
16.         if (best double-point part-line is found)
17.         {
18.            Partition object using best double-point part-line;
19.            Filter concave points and part-lines lists;
20.            Assign concave points and part-lines lists to the two new objects;
21.            Push the two new objects into stack;
22.         }
23.         else // best double-point part-line is not found
24.         {
25.            Push the object into stack;
26.         }
27.      }
```

```
28.     else if (concave points list is not empty)
29.     {
30.         Find best single-point part-line;
31.         if (best single-point part-line is found)
32.         {
33.             Partition object using best single-point part-line;
34.             Filter concave points and part-lines lists;
35.             Assign concave points and part-lines lists to the two new objects;
36.             Push the two new objects into stack;
37          }
```

negative curvature minima

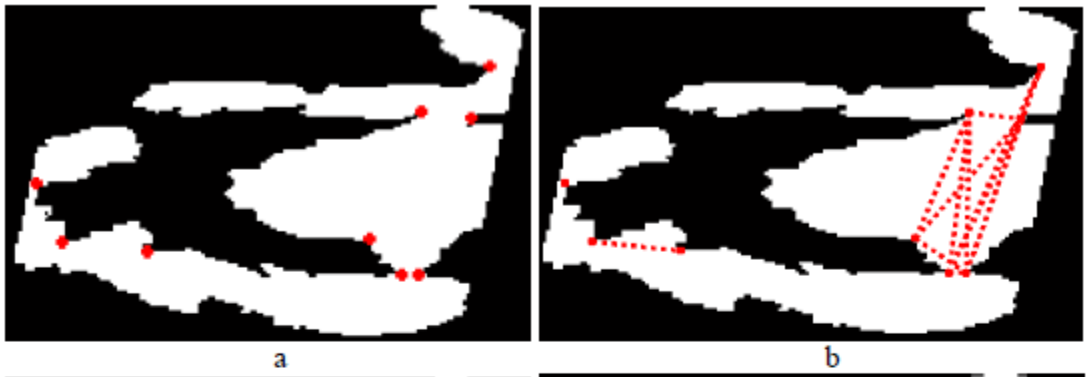

double-point part-lines

enclosing circle of a part-line not within object

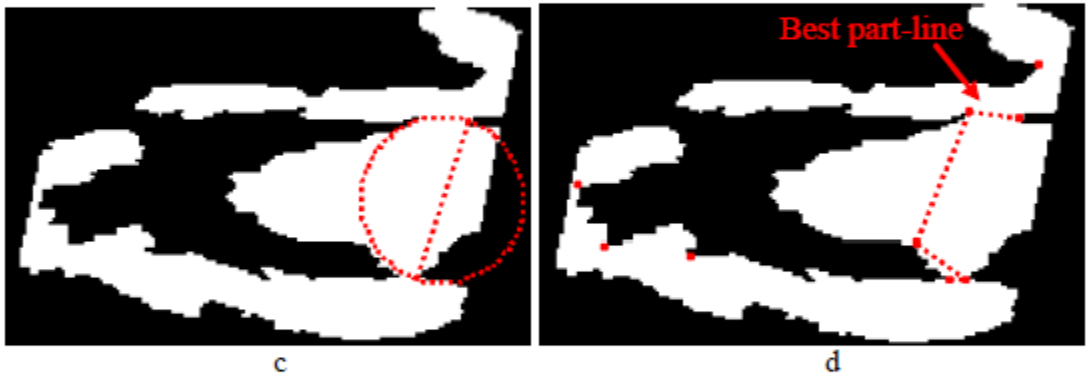

filtered double-point part-lines

two single-point part-lines associated with a concave point

first partition with best part-line that results in a maximum eccentricity part

filtered lists of points & part-lines

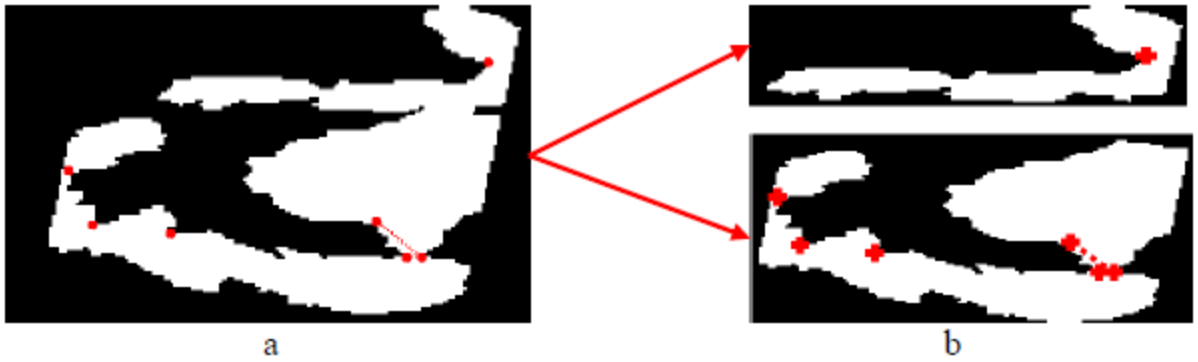

two new parts with associated points and double-point part-lines

a part with double-pnt part-line

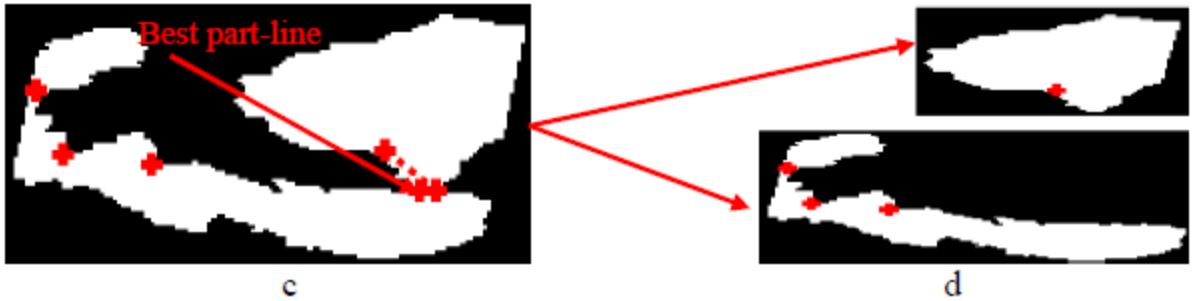

two new parts from lower one

object partition after consuming all double-point part-lines

final object partition

Results on Other Frames

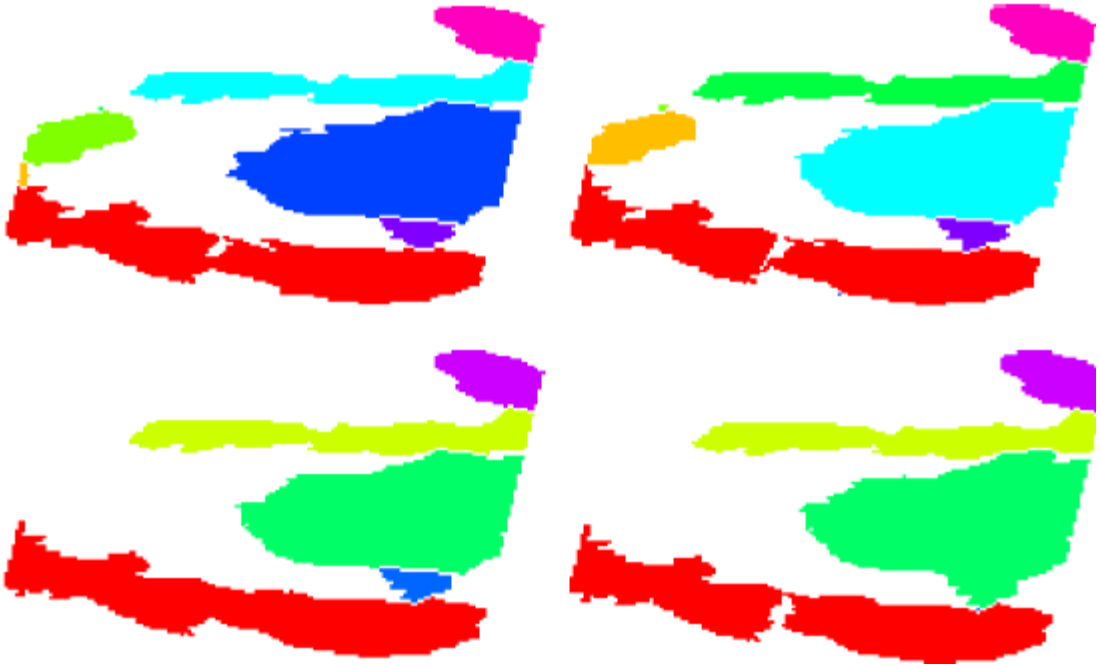

More Vessel Segmentation Results

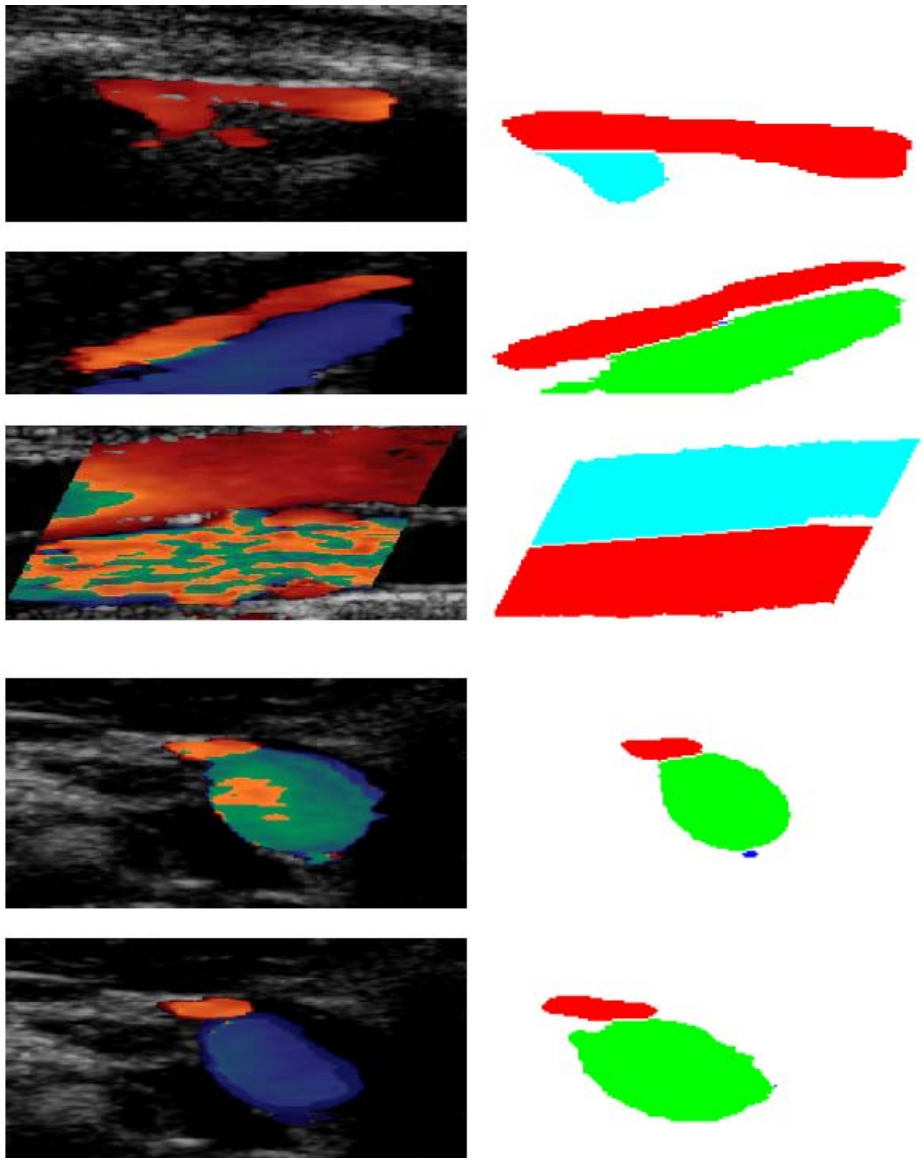

More Vessel Segmentation Results

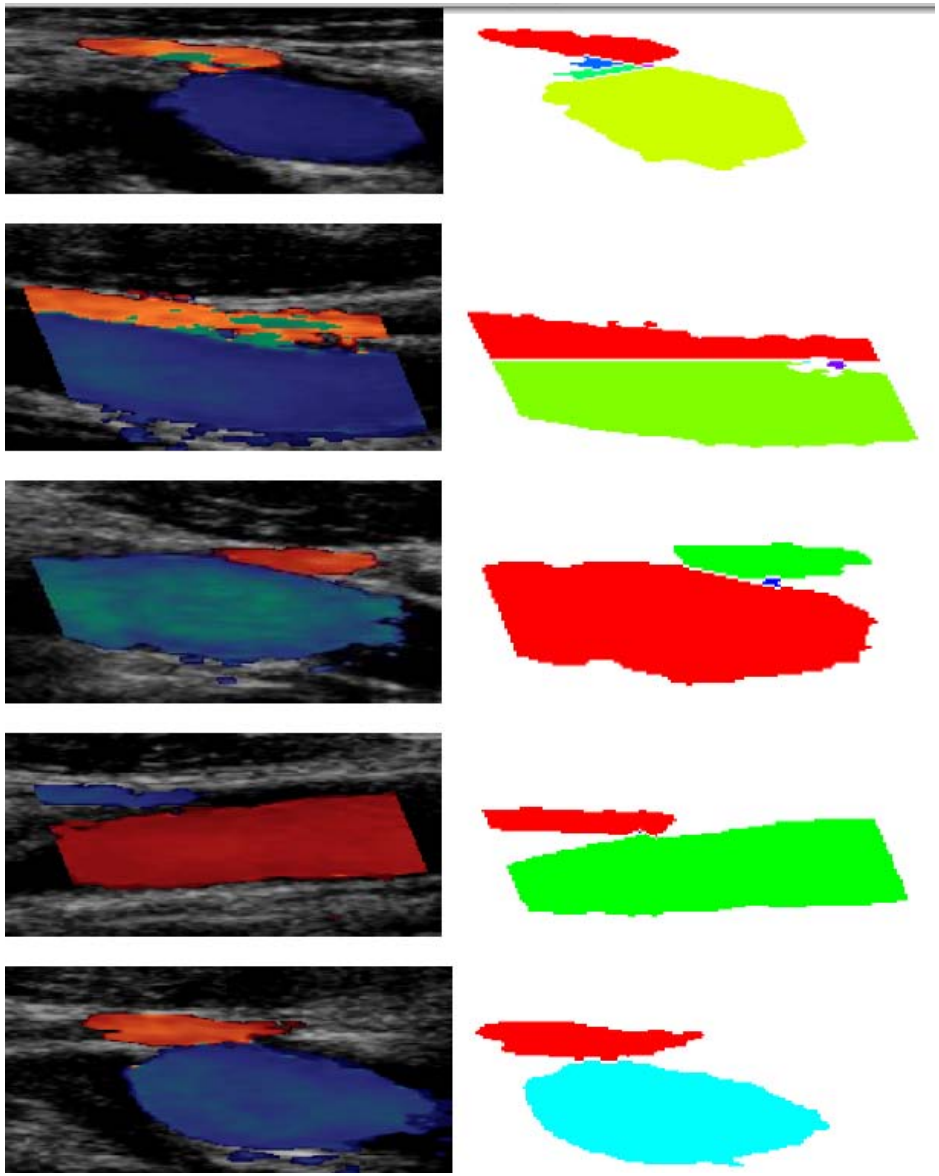

Vessel Segmentation Clinical Application - Automatic Doppler Angle Determination

- Ultrasound systems offer a graphical user interface that the user can move anywhere over the image to locate the line center over the vessel's site of interest.
- The user can rotate a knob to align the line with the vessel axis.
- The ultrasound system software internally uses the position provided by the user to acquire Doppler spectrum signals while it uses the angle to calculate the blood flow velocity.

- The two main drawbacks of the manual technique are
  - time consumed
  - angle inaccuracy

- The new vessel segmentation results allows accurate automation of the Doppler angle computation using the skeletonization of the segmented vessels.

- The Doppler angle is estimated as the best line fit of the skeleton pixels around the Doppler gate*.

*The Doppler gate is the point of interest inside a blood vessel that the user specifies to acquire the Doppler data from.

Doppler Angle Automation Results

- The green square represents the Doppler gate position.
- The white line represents the automated Doppler angle.

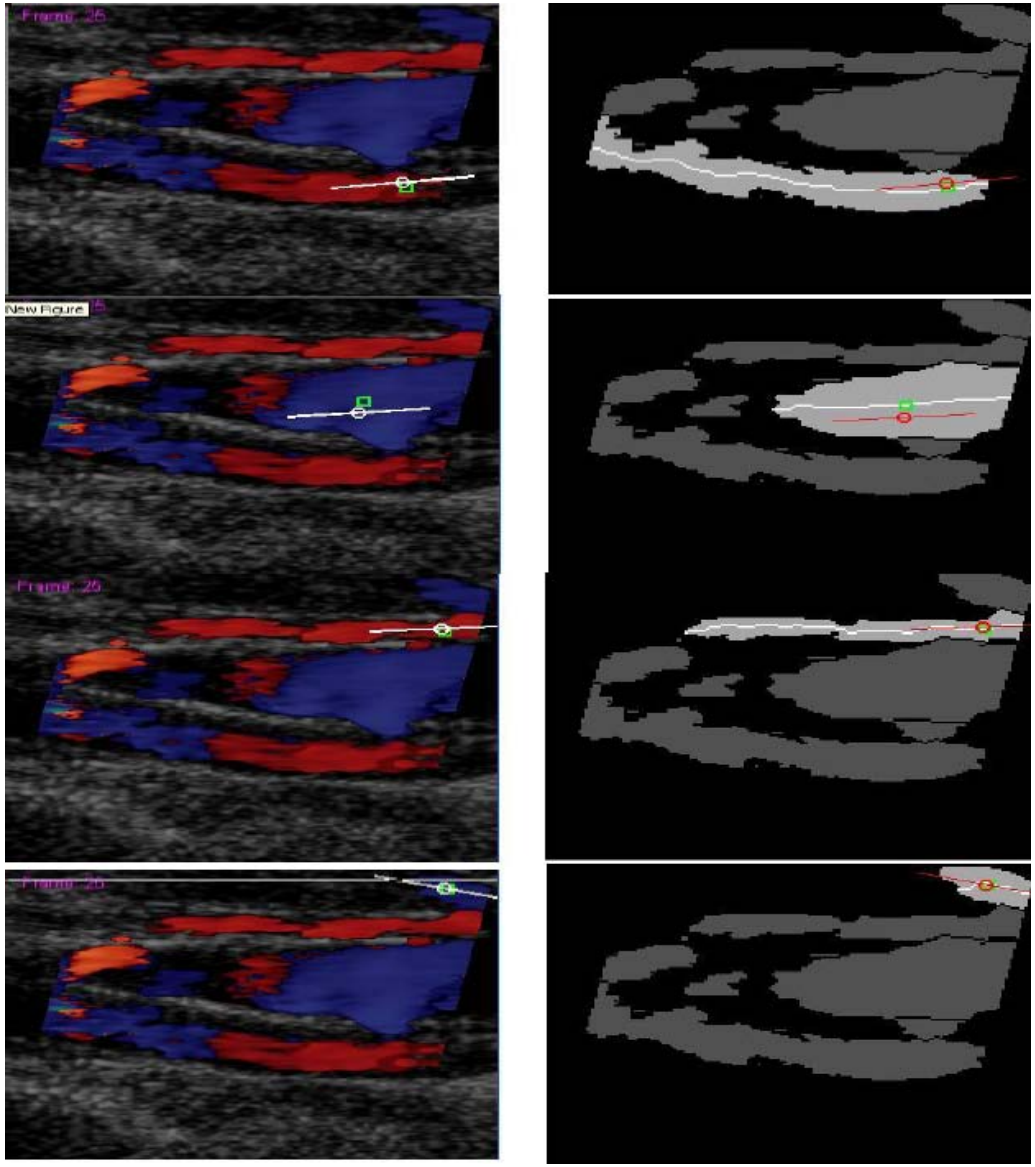

Bland-Altman Analysis

- Bland-Altman analysis is a popular method in medical statistics for evaluating the agreement between two measurements.

- It plots the difference of the two methods against the mean of the two. If the differences are small, the methods agree.

Doppler Angle Automation Statistical Validation – Matlab Simulations

- Validating the angle automation against the gold standard: expert manual angle settings
- Offline ultrasound color Doppler images were produced by expert sonographers from Philips Ultrasound.
- Matlab GUI application was developed to allow manual expert angle estimation.
- Automated angle estimation was calculated for the same manual Doppler gate positions.
- Statistical regression and Bland-Altman analysis were conducted, showing strong correlation between manual and automated angle settings.
  - Correlation coefficient = 0.97
  - Angle differences mean = -0.93˚
  - Angle differences standard deviation = 5.4 ˚

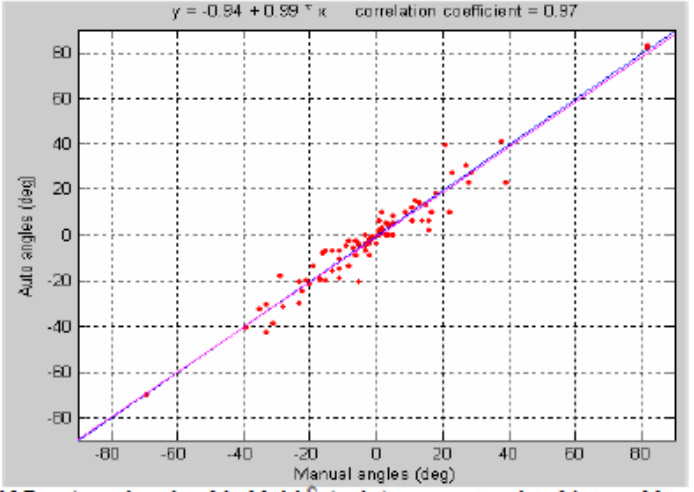

Figure 3.15 Experimental results of the Matlab© simulation. x-y scatter plot of Auto vs. Manual angles, plus identity line (blue), and least-squares-line (magenta).

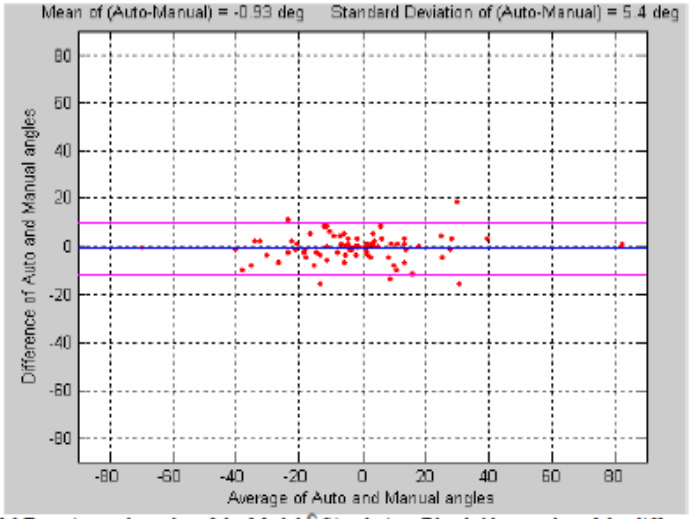

Figure 3.16 Experimental results of the Matlab© Simulation. Bland-Altman plot of the difference of the Auto and Manual angles vs. the average of the Auto and Manual angles, plus mean of differences (blue), and mean ± two standard deviations of differences (magenta).

Doppler Angle Automation Statistical Validation – Real-time Prototype

- The vessel segmentation and Doppler angle automation applications were prototyped on the Philips iU22 ultrasound system using C++ code.
- Expert sonographers conducted manual Doppler angle settings on model volunteers.
- Automated Doppler angle was triggered using a system button after the manual setting.
- Statistical regression and Bland-Altman analysis were conducted, showing strong correlation between manual and automated angle settings:
  - Correlation coefficient = 0.99
  - Angle differences mean = 1.66˚
  - Angle differences standard deviation = 6.44 ˚

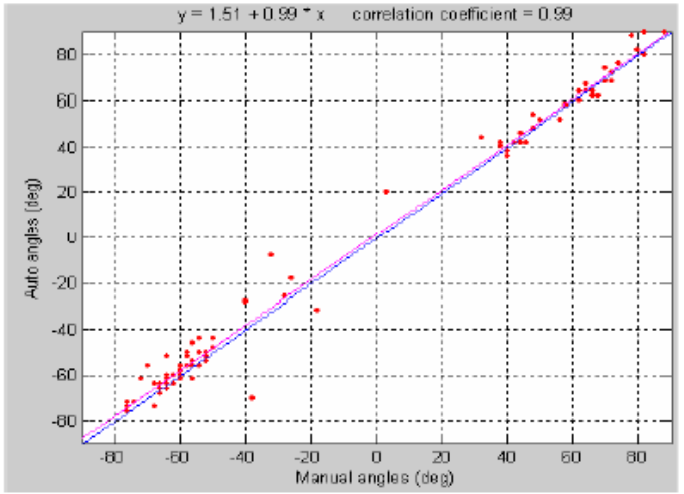

Figure 3.17 Experimental results of the real-time prototype. x-y scatter plot of Auto vs. Manual angles, plus identity line (blue), and least-squares-line (magenta).

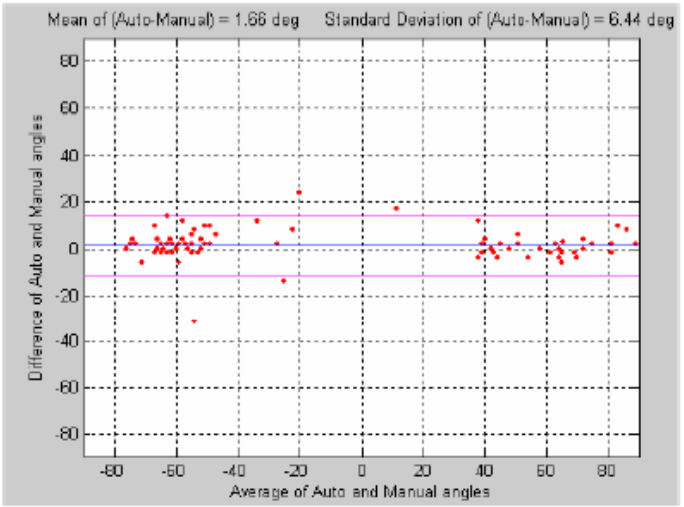

Figure 3.18 Experimental results of the real-time prototype. Bland-Altman plot of the difference of Auto and Manual angles vs. the average of Auto and Manual angles, plus mean of differences (blue), and mean ± two standard deviations of differences (magenta).

Color Doppler Aliasing Artifact and Phase Unwrapping Techniques

- Color Doppler ultrasound is a powerful non-invasive blood vessel diagnostic tool, but it is still mainly a qualitative tool.
- Components of the signal's spectrum with frequencies greater than twice its frequency will appear to lie at different places on the spectrum than they actually are.
- This **aliasing** artifact is the main source of distortion of color Doppler images and occurs when the pulse repetition frequency (PRF) is not high enough to sample the highest blood velocity.
- Our research goal is to recover the true velocities from the aliased ones in order to facilitate advanced quantification and image analysis tasks.
- The color Doppler image is treated as a phase map, and the unaliasing problem is formulated as a phase unwrapping problem.

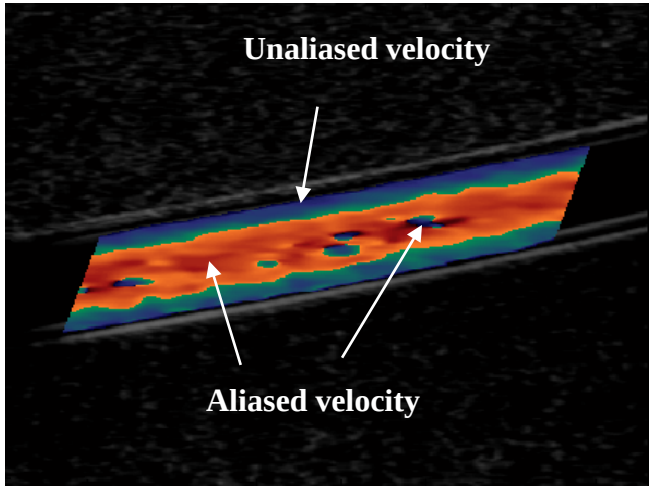

An aliased color Doppler image of a flow phantom

Fringeline Tracking for Phase Unwrapping

- Velocity aliasing is a common artifact in color Doppler ultrasound imaging
- The aliasing artifact occurs when the sampling frequency used to acquire images is not high enough to unambiguously sample the highest blood flow velocity within the imaged vessels.
- The artifact manifests itself as high velocity pixels that appear to have reverse flow velocities.

Color Doppler Aliasing Example

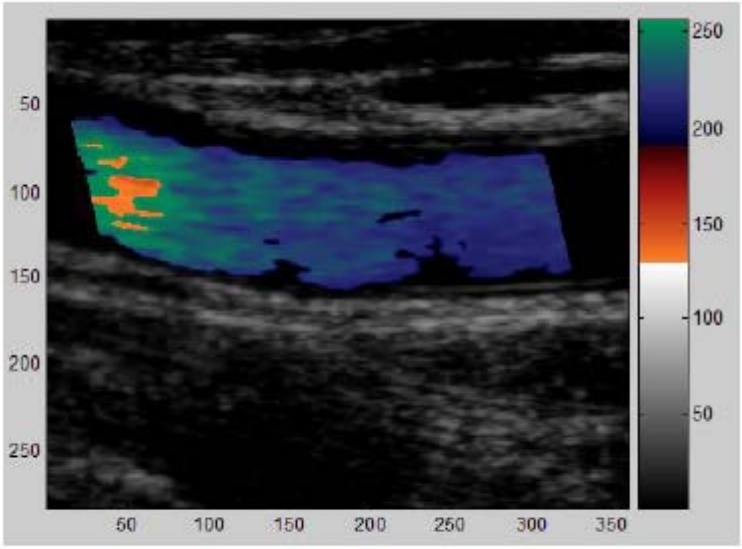

Figure 4.2 A color Doppler ultrasound image of the proximal common carotid artery. The unaliased velocity pixels are shown in blue while the aliased velocity pixels are shown in red.

Phase Unwrapping Theory

The wrapping process is a nonlinear process.

$$\psi(\omega) = \varphi(\omega) + 2\pi k(\omega) = W(\varphi(\omega))$$

Wrapped phase within interval $(-\pi, \pi]$

True phase

Integer function

Mapping operator

The unwrapped phase can be calculated recursively by integrating the wrapped phase differences.

$$\varphi(m) = \varphi(0) + \sum_{n=0}^{m-1} W(\nabla(\psi(n))$$

Gradient operator

Under the condition of phase continuity.

$$-\pi < \nabla(\varphi(n)) < \pi$$

Relationship between True Phase and Wrapped Phase

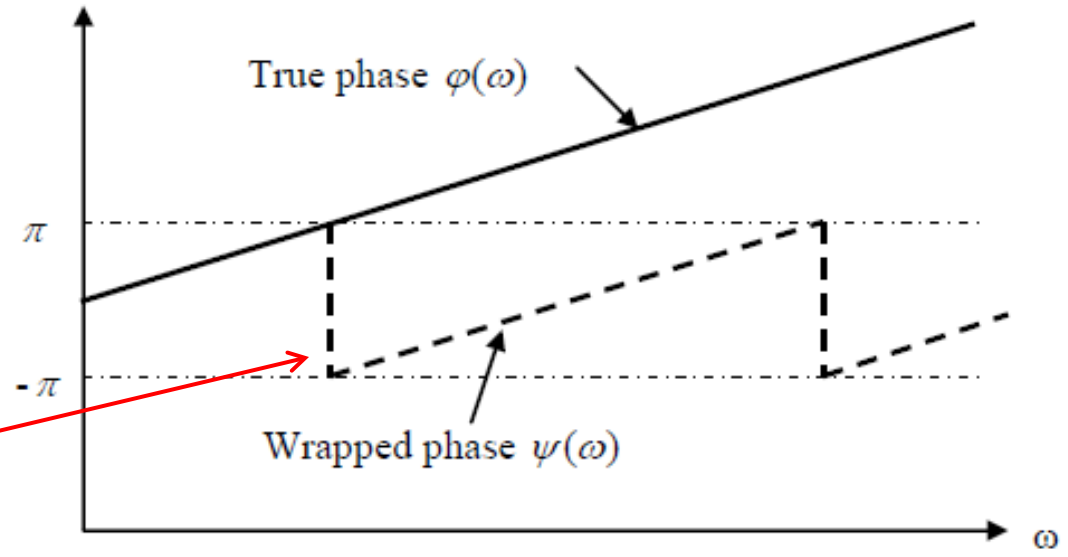

discontinuity

Figure 4.6 The relationship between the true phase $\varphi(\omega)$ and the wrapped phase $\psi(\omega)$.

Phase Unwrapping Theory – cont.

The phase continuity condition can be violated due to undersampling, noise, or nonlinear signal processing.

Traces of phase discontinuity can be easily detected.

- sum phase around each 2x2 square
- if sum = 0, no discontinuity
- if sum = 2π, positive residue (+)
- if sum = -2π, negative residue (o)

Discontinuities were flagged with non-zero value phase integrals. Phase discontinuity points are called "**Residues**".

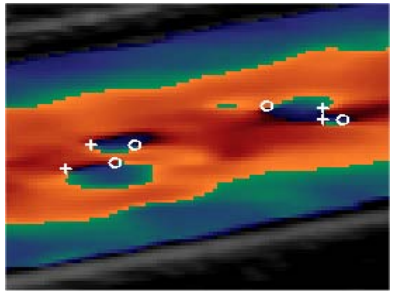

Phase discontinuity residues

Ignoring phase residues during unwrapping will cause unwrapping errors to propagate.

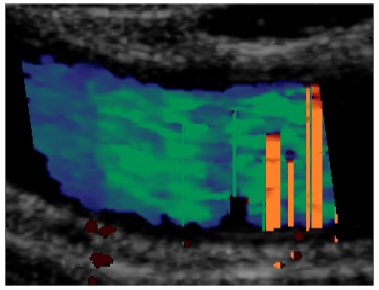

Phase unwrapping errors

Tests of Existing Algorithms: Data Acquisition Protocol

• Captured color Doppler cineloops that encompass at least one heart cycle.

• Both flow phantom simulated waveforms and in-vivo peripheral vascular cases were captured.

• Some acquisition controls had to be fixed to minimize distortion:

- Temporal averaging "**color persistence**" is turned off.
- **Clutter filter** is set to minimum setting.
- **Spatial smoothing** is set to minimum setting.

• The color scale or **PRF is swept** from very high settings to very low settings to generate unaliased, moderately-aliased, and severely-aliased cases.

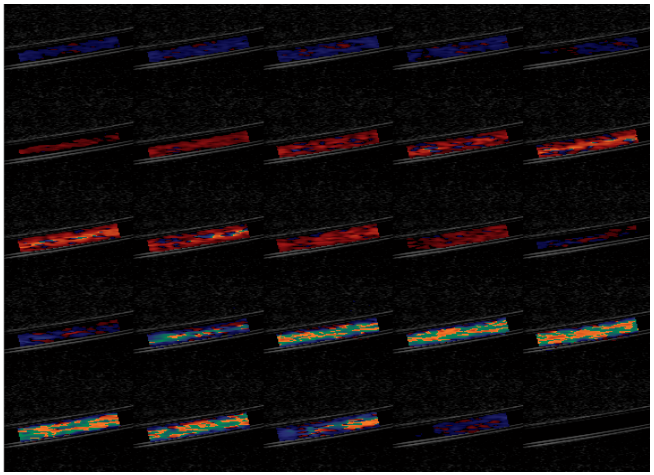

Flow phantom femoral dataset

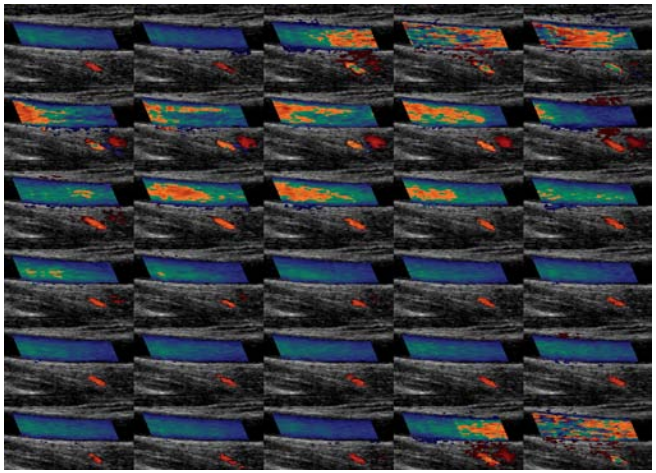

In-vivo carotid dataset

Tests of Existing Algorithms:

Performance with Color Doppler Ultrasound Images

Goldstein's branch-cut introduced wrong residue connections.

Flynn's mask-cut algorithm's quality maps did not always agree with the correct residue dipole connections.

Flynn's min. discontinuity algorithm performed the best. However unwrapping errors occurred and the algorithm is slow.

Unwrapping errors are more severe with minimum normalization methods, including DCT and PCG algorithms.

The existing algorithms achieve **consistent**, but not necessarily **accurate** results.

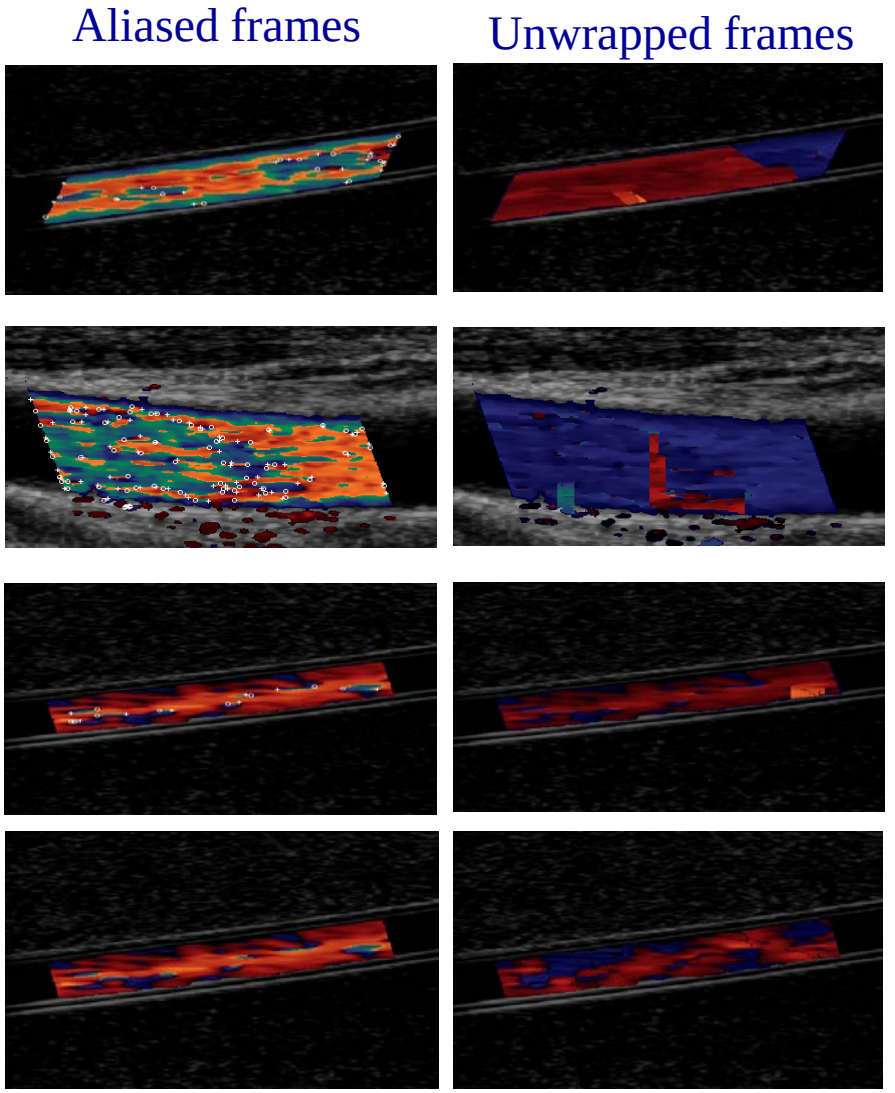

The New Fringeline-Tracking Approach

Recently, some algorithms sought accurate phase unwrapping results for MRI based on the detection of **true phase discontinuity** cutlines.

Cutlines are borderlines between adjacent pixels where the modulus of the true phase variation gets larger than π.

Fringelines are borderlines between two adjacent pixels where phase wrapping occurs (2π jumps).

Residues are the intersection points between cutlines and fringelines.

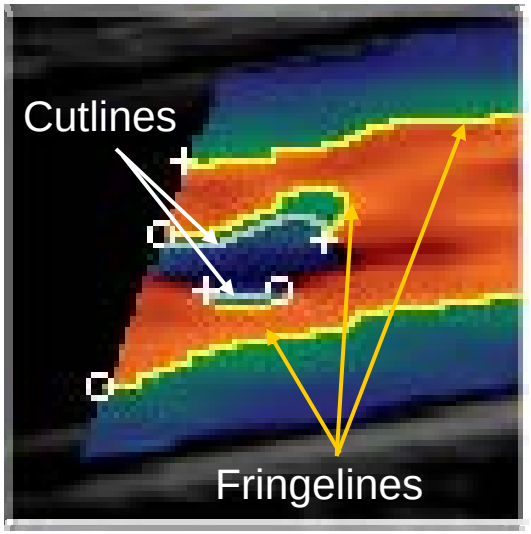

Introducing **phase shift** to the image causes the fringelines to shift, but the cutlines will not shift.

Proposed methods find **portions** of the hidden cutlines as the union of **many** intersecting phase shifted fringelines, or the ridges of the superpositioned phase shifted fringelines.

The New Fringeline-Tracking Approach – cont.

The clinically useful range for color Doppler phase unwrapping is (- 3π, 3π].

The pixels can be classified as: unaliased, moderately-aliased, and severely-aliased.

Phase discontinuity occurs between unaliased and severely-aliased regions.

Nearby the phase discontinuity regions, the unwrapped pixels tend to cluster around π, while the severely-wrapped pixels tend to cluster around 0.

The logical threshold that can separate the two clustered regions is the fringeline associated with the π/2 (or - π/2) phase shift.

The π/2 (or - π/2) fringelines guide the coupling of the opposite-sign residues.

Heuristic information is used to select one of the two unwrapping solutions.

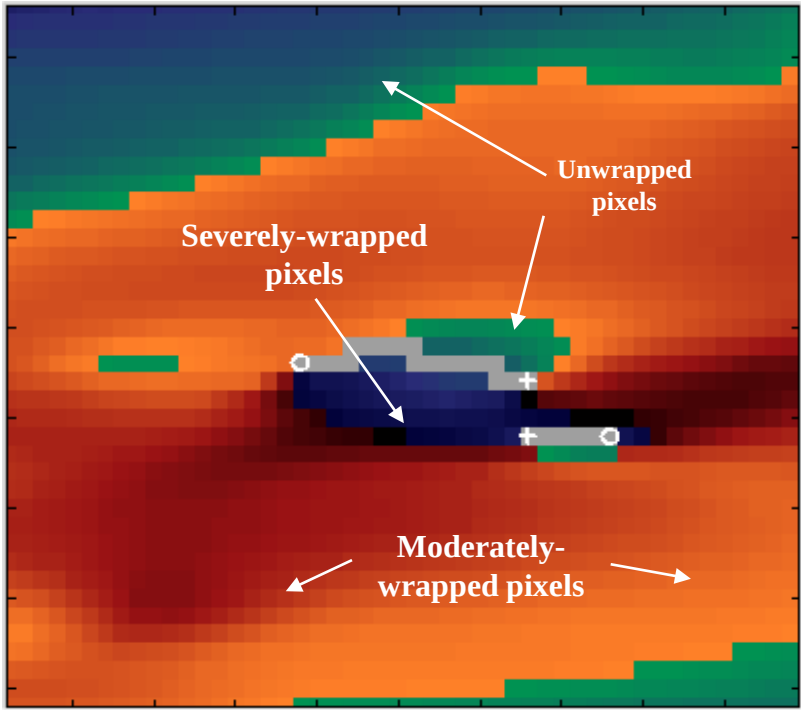

The New Fringeline-Tracking Unwrapping Results

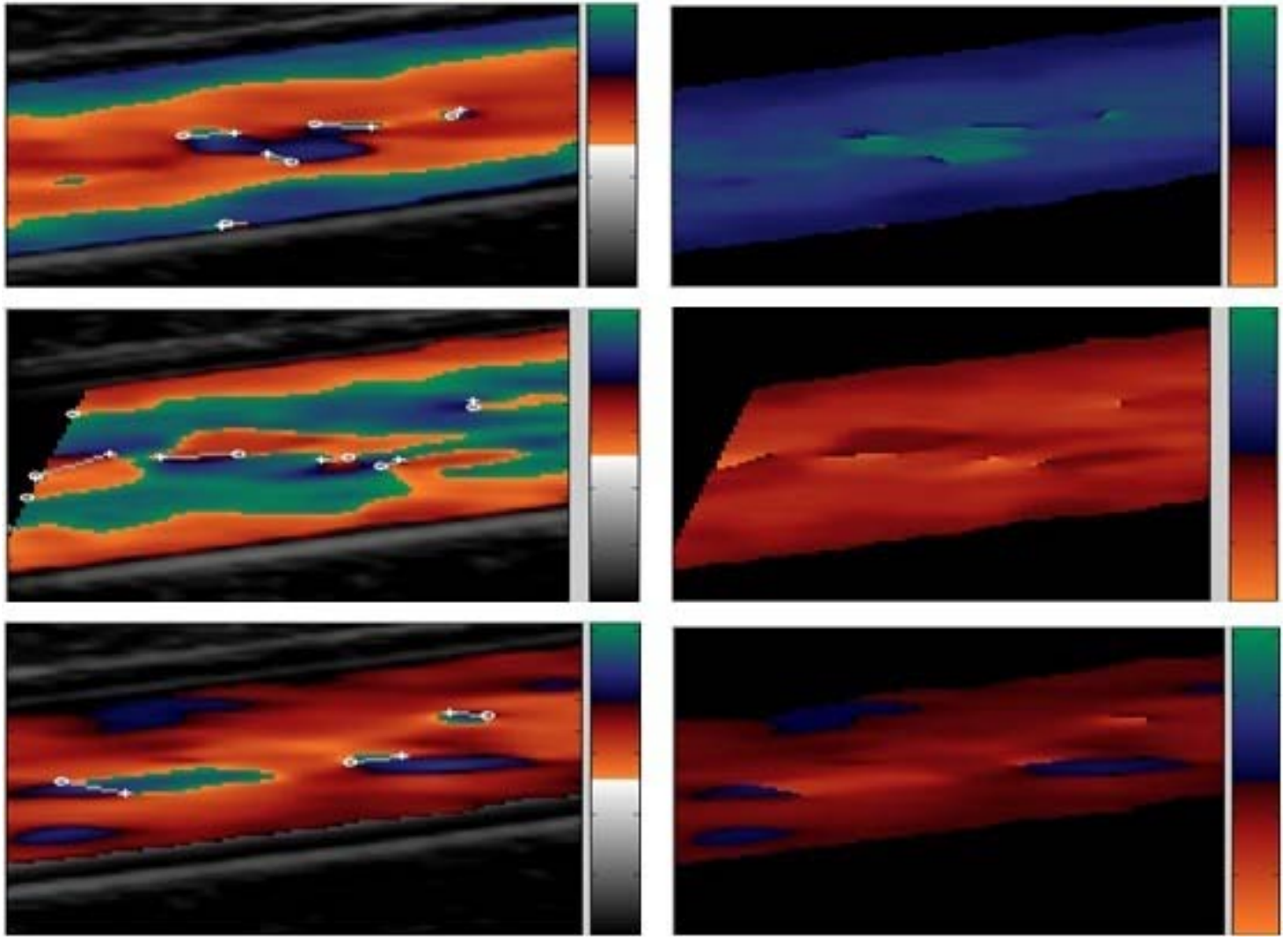

Aliased frames

Unwrapped frames

Results Validation

Qualitative validation based on heuristic information about the underlying vessel:

- Pulsatility: heart pulsation
- Phasicity: related to heart cycle
- Flow direction: toward or away from ultrasound transducer
- PRF and peak velocity: max velocity of the blood within the vessel

If successful, the pulsatility, phasicity and direction should be maintained.

Quantitative validation based on the maximum velocity estimation from the unwrapped cineloops. The estimated max velocity should match across the sweeping PRF (Pulse Repetition Frequency).

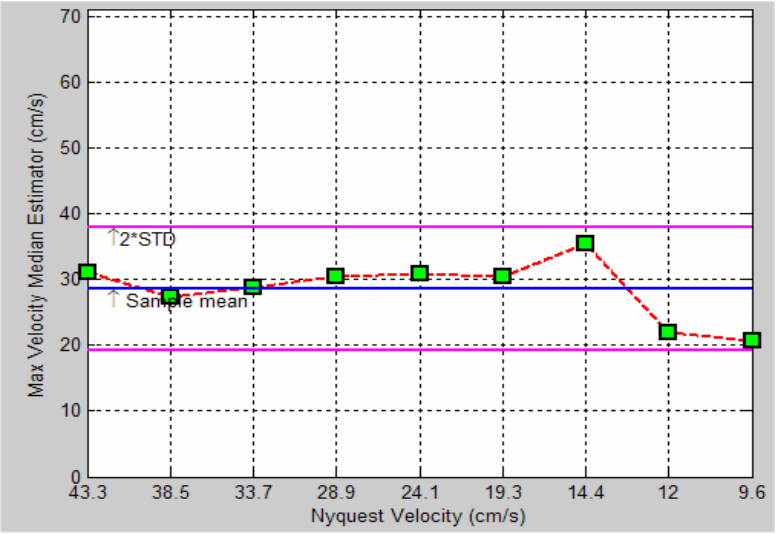

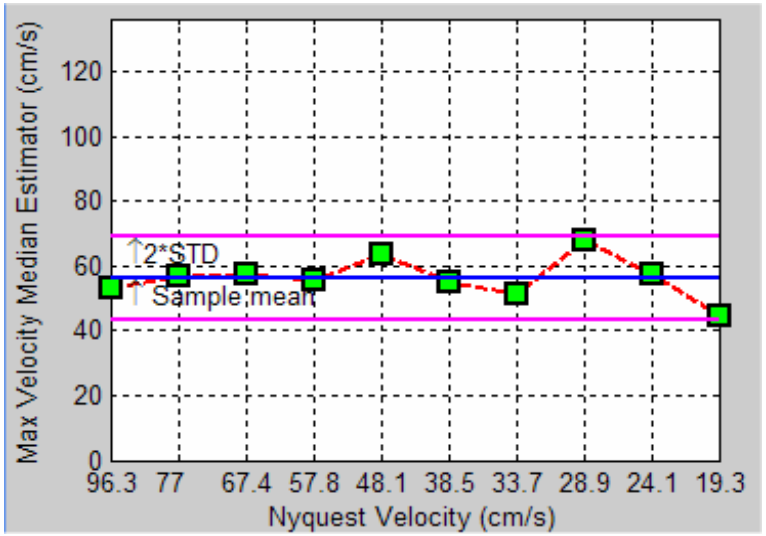

Results Statistical Analysis

	#Images	New Fringeline-tracking	Goldstein's Branch-cut	Flynn's Mask-cut	Flynn's Min. Disc.	Giglia's DCT	Giglia's PCG
All aliased	259	253	212	227	238	214	193
Success rate %		98%	82%	88%	92%	83%	75%
Severely-aliased	66	62	45	54	58	54	38
Success rate %		94%	68%	82%	88%	82%	58%

Phase unwrapping success rates for all algorithms

Phase Unwrapping Conclusions

- The color Doppler aliasing problem was addressed and a new phase unwrapping technique was developed.
- The results should open the door for more advanced quantification and image analysis applications.
- The phase unwrapping results constitute a building block of a vessel recognition system based on the analysis of color Doppler ultrasound images.

Vessel Feature Generation

- After the preprocessing steps of the recognition system (vessel segmentation and phase unwrapping), the next task is the vessel feature extraction.

- Generation of input data for the recognition system involved:
  - Histogram-based data reduction methodology
  - Data preprocessing to achieve invariance under several transformations
  - Transform-based feature extraction methods

Data Acquisition Protocol

- In order to run controlled experiments, a Doppler flow phantom was used for the data acquisition.
- Five different waveforms typically found in human vessels were used as a case study:
  - carotid
  - constant
  - femoral
  - sinusoidal
  - square

carotid

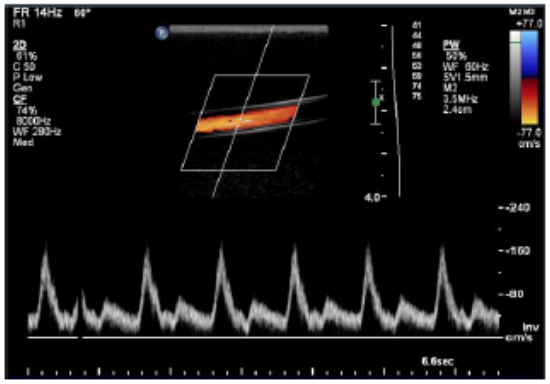

(a)

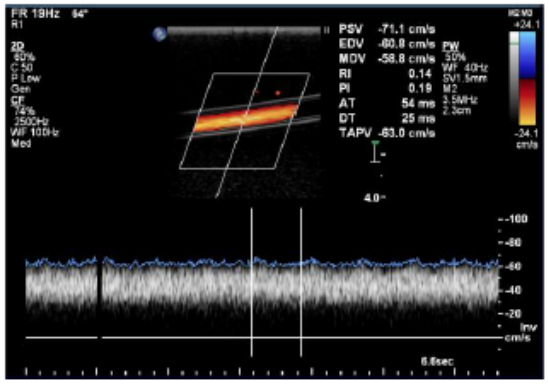

(b)

constant

femoral

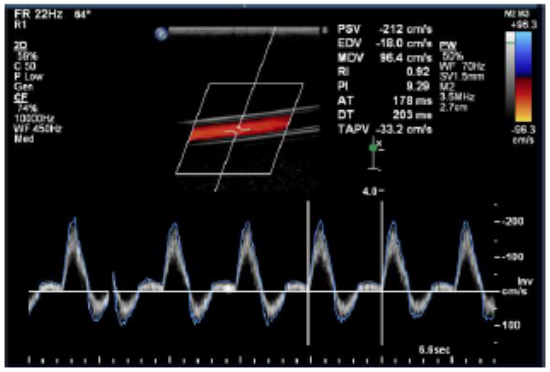

(c)

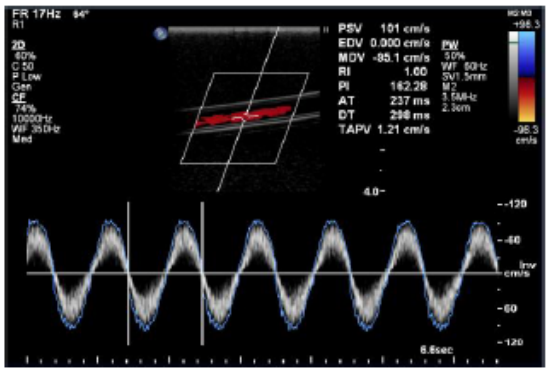

(d)

sinusoidal

square

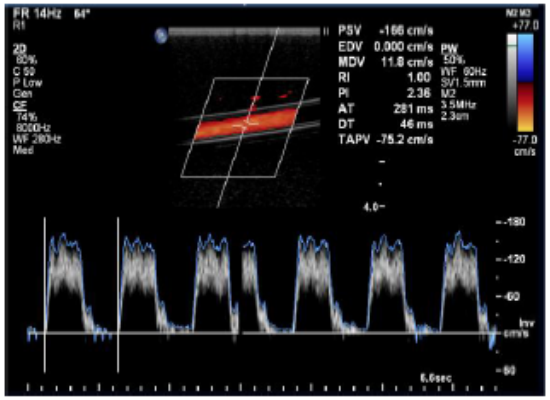

(e)

Processing

- First phase unwrapping was applied
- Next dimensionality reduction was performed on the unwrapped color Doppler data, while maintaining the temporal signature of the underlying vessel.
- This signature can be used directly or through transformations by the recognition system without attempting to extract additional discrete features.

Color Doppler Virtual Spectrogram

Discretized Velocity

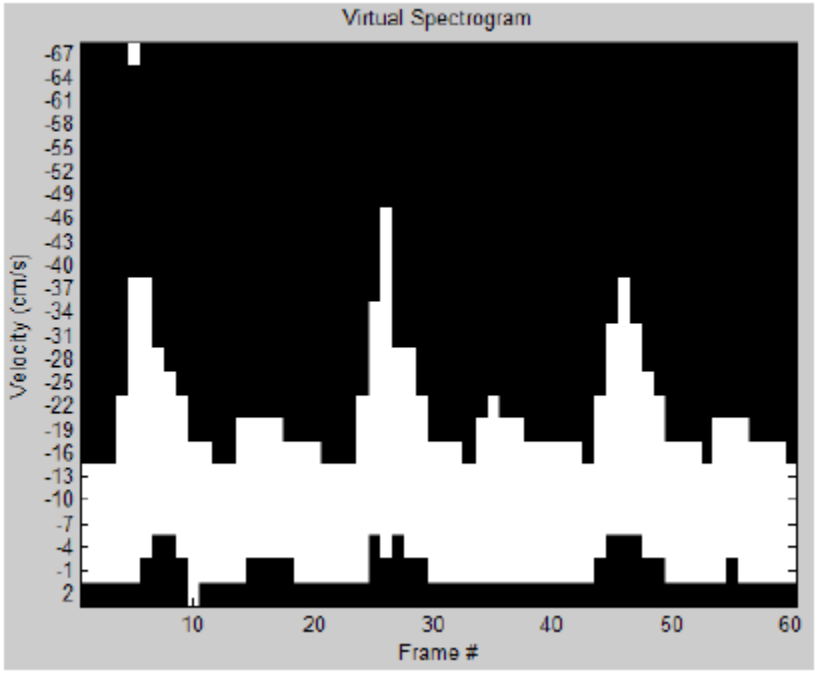

Frame Number

Virtual Spectrograms for Carotid Waveform with Different Steering Angles

20°

16°

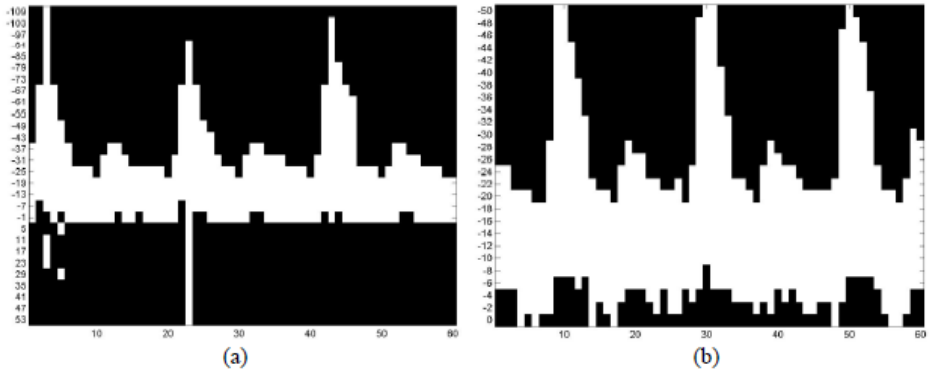

12°

8°

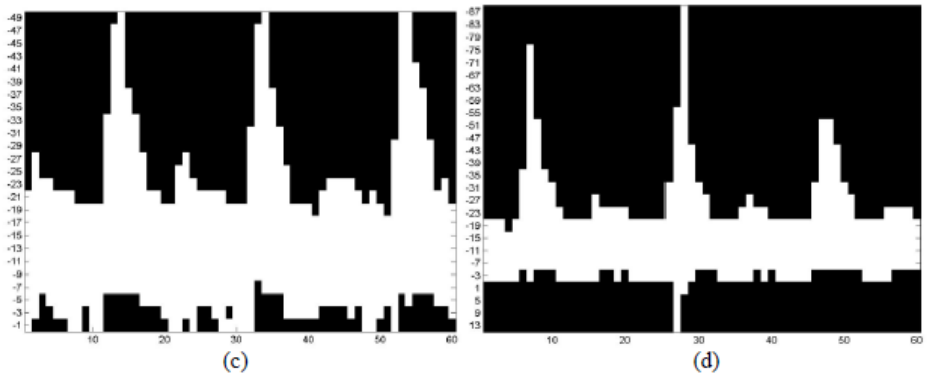

4°

0°

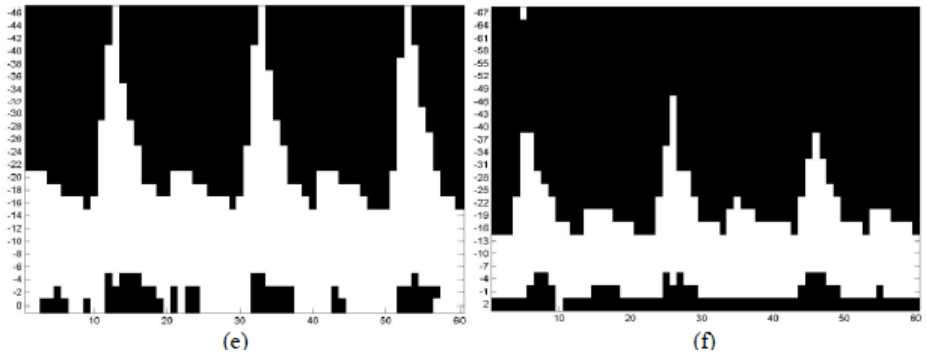

Virtual Spectrogram Profile

- The relevant data in the Virtual Spectrogram that discriminates between vessels is found at its boundary.
- The boundary is extracted to form the Virtual Spectrogram Profile (VSP)

blue line is raw VSP
red line is median filtered VSP

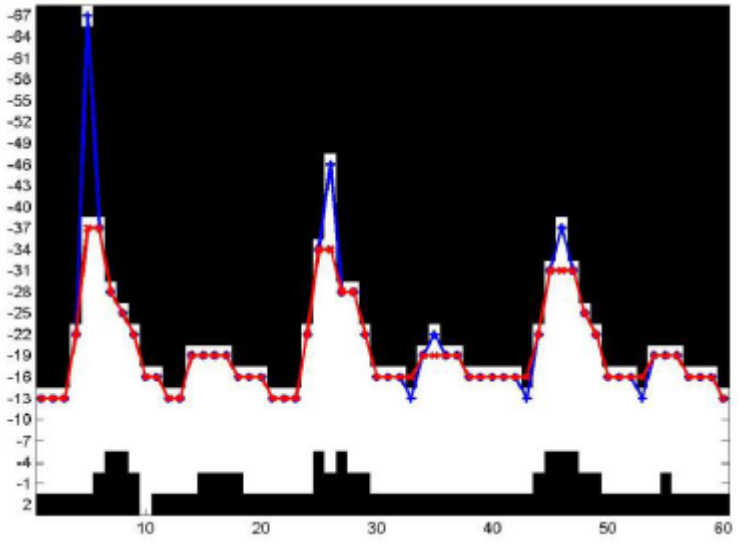

VSP (cont)

- A single pitch (period) of the waveform is detected.
- Shift-invariance normalization is applied.
- Sample-size invariance normalization is applied.
- Scale invariance normalization is applied.
- Three kinds of transform-based features were explored
  1. Fourier descriptors
  2. Wavelet descriptors
  3. Moment descriptors

Classification Experiments

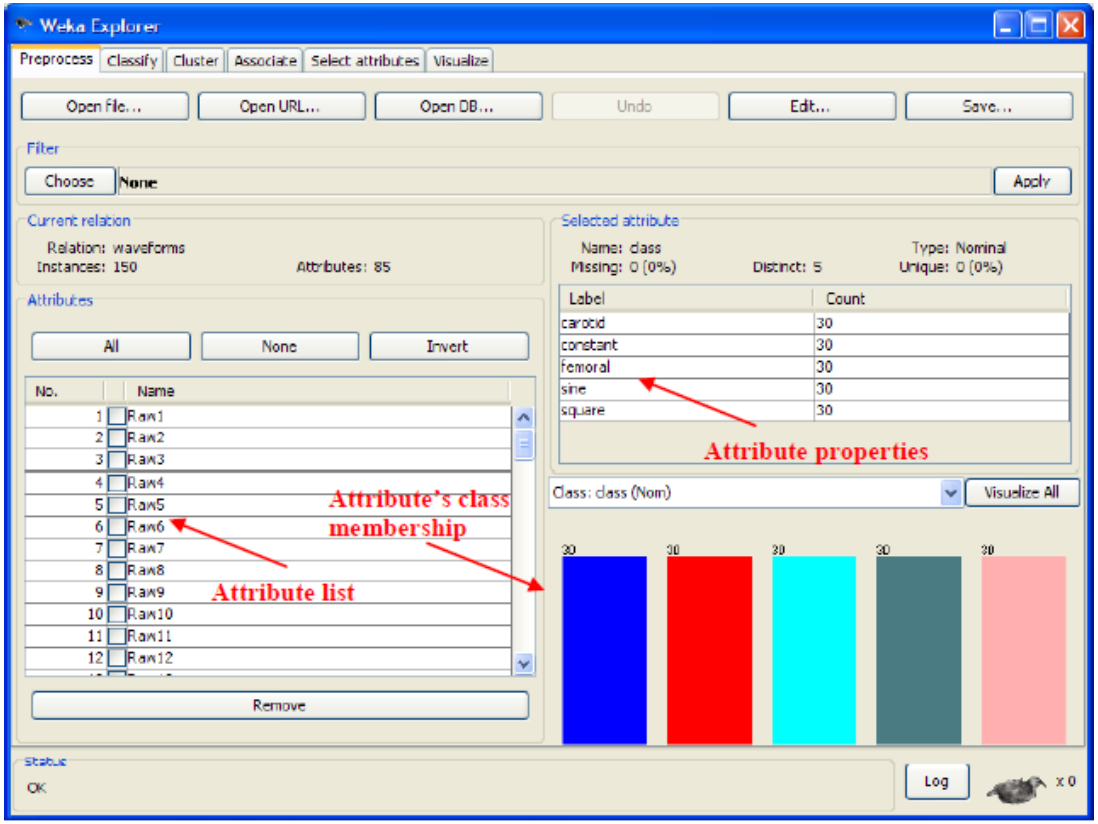

The WEKA Explorer interface was used to try out multiple different classifiers and features.

Classification Success Rates of Different Preprocessing Methods

	No scaling/ variant descriptors	No scaling / invariant Descriptors	Lost-sign scaling/ variant descriptors	Preserved-sign scaling/ variant descriptors
Raw (32)	96.0%	NA	90.0%	97.3%
FD (5)	73.3%	77.1%	85.3%	94.6%
WD (16)	96.6%	97.3%	86.6%	98%
MD (5)	60.6%	68%	60.6%	95.3%

Table 7.3 Classification success rates for using TRAINING1 set as a training set while TEST1 and TEST2 sets are used as test sets.

	TRAINING1	TEST1	TEST2
Raw (32)	97.3%	94.4%	87%
FD (5)	94.6%	91.1%	67.3%
WD (16)	98%	94.9%	90.3%
MD (5)	95.3%	93.7%	69.7%

Table 7.4 Classification success rates for using TEST1 set as a training set while TRAINING1 and TEST2 sets are used as test sets.

	TEST1	TRAINING1	TEST2
Raw (32)	96.8%	95.3%	70.9%
FD (5)	95.9%	92.7%	69.7%
WD (16)	96.4%	95.3%	71.2%
MD (5)	93%	91.3%	65.8%

Table 7.5 Classification success rates for using TEST2 set as a training set while TRAINING1 and TEST1 sets are used as test sets.

	TEST2	TRAINING1	TEST1
Raw (32)	94.2%	94.6%	92%
FD (5)	81.8%	90%	89%
WD (16)	94.5%	94.7%	91.5%
MD (5)	88.5%	83.3%	80.5%

Some of the Conclusions

- The raw and wavelet descriptors were consistently superior to the Fourier and moment descriptors.
- This was true for all 10 classifiers with negligible differences.
- All classifiers performed statistically better than Naive Bayes.
- The Random Forest classifier gave the best performance with all four descriptors.